

Interpretable Multi-task Learning with Shared Variable Embeddings

Maciej Żelaszczyk¹

Jacek Mańdziuk^{1,2}

¹Faculty of Mathematics and Information Science, Warsaw University of Technology, Poland

²Faculty of Computer Science, AGH University of Krakow, Poland
m.zelaszczyk@mini.pw.edu.pl, jacek.mandziuk@pw.edu.pl

Abstract

This paper proposes a general interpretable predictive system with shared information. The system is able to perform predictions in a multi-task setting where distinct tasks are not bound to have the same input/output structure. Embeddings of input and output variables in a common space are obtained, where the input embeddings are produced through attending to a set of shared embeddings, reused across tasks. All the embeddings are treated as model parameters and learned. Specific restrictions on the space of shared embeddings and the sparsity of the attention mechanism are considered. Experiments show that the introduction of shared embeddings does not deteriorate the results obtained from a vanilla variable embeddings method. We run a number of further ablations. Inducing sparsity in the attention mechanism leads to both an increase in accuracy and a significant decrease in the number of training steps required. Shared embeddings provide a measure of interpretability in terms of both a qualitative assessment and the ability to map specific shared embeddings to pre-defined concepts that are not tailored to the considered model. There seems to be a trade-off between accuracy and interpretability. The basic shared embeddings method favors interpretability, whereas the sparse attention method promotes accuracy. The results lead to the conclusion that variable embedding methods may be extended with shared information to provide increased interpretability and accuracy.

1 Introduction

The ability to extract common information from varied settings has long been one of the central challenges in machine learning. The degree to which the considered domains differ and the complexity of the domains themselves has grown considerably over time. Artificial neurons [24] linked in a physical perceptron model [34] were used to distinguish, through a weight update procedure, the side on which a punch card had been marked. CNNs [13, 21] are able to identify similar patterns in distinct areas of an image. Word embeddings [4, 28] have been used to obtain representations fusing information from different contexts. Reinforcement learning agents achieved relatively high performance in a number of Atari games without changes to the model architecture [30]. Generative methods, such as diffusion models [33] produce high-fidelity imagery based on information from a provided text prompt.

Multi-task learning (MTL) is a specific area of machine learning concerned with approaches that attempt to simultaneously solve more than one task [6–8, 35, 9]. With the evolution of deep learning architectures over the years, we have seen a sharp increase in the interest in MTL, e.g. in hard parameter sharing methods [19, 11], soft parameter sharing methods [29, 14], decoder models [5, 39]. MTL also has strong links to *self-supervised learning* (SSL) — a learning paradigm where models

can be pretrained on unlabelled data in order to improve their performance or data efficiency on downstream tasks [28, 10, 40, 3, 1].

MTL and SSL can be interpreted as settings in which knowledge about one task facilitates the learning of another one. This is usually done via a choice of tasks that share significant structure, e.g. semantic segmentation, human parsing, monocular depth estimation, etc. This is in stark contrast to real-world prediction scenarios, where typically no a priori structure is given. The difficulty in obtaining meaningful structure from unrelated tasks has led research on MTL to mostly focus on related tasks, even though there is a body of work suggesting that solving not obviously related tasks may actually be helpful in making sound predictions [22, 26].

A specific line of investigation for tabular data postulates casting variables associated with unrelated tasks into a shared embedding space, on top of simply measuring the value of these variables [27]. This can also be understood as associating with each variable a (key, value) pair, where the key is a *variable embedding*. This draws inspiration from word embeddings [4], attention [2, 38] and key-value retrieval methods [16, 17, 15]. Such an approach affords to perform classification or regression and to tackle distinct tasks with different numbers of inputs and outputs in order to extract unobvious common information. It does, however, require each variable to be assigned a unique embedding. This limits the ability to reason about the degree to which specific variables are similar to one another and about their shared components.

This paper aims to investigate the extent to which variable embeddings can reuse the same information and proposes a setting where each variable embedding can be represented as a reconfiguration of a common component base shared across tasks. This, in turn, allows us to link any common component to specific variables which rely on it most and to identify common concepts shared between variables.

Motivation: We aim to: (1) encourage information re-use by relaxing the assumption of one VE per variable, (2) facilitate interpretability in the VE setting, (3) verify whether restrictions on the shared information improve the accuracy and training efficiency of the VE method.

Main contributions of this paper:

- Proposes a variable embedding architecture with a shared component base accessed via attention.
- Shows that the introduction of the shared base does not hurt performance, while allowing for a substantial reduction in training steps.
- Verifies that specific components from the shared base incorporate abstract intuitive concepts.
- Investigates specific restrictions on the form of the shared base and the attention mechanism.
- Identifies and investigates the trade-off between interpretability and accuracy in shared embedding systems.

2 Background

We consider a setting with T tasks $\{(\mathbf{x}_t, \mathbf{y}_t)\}_{t=1}^T$, where task t has n_t input variables $[x_{t1}, \dots, x_{tn}] = \mathbf{x}_t \in \mathbb{R}^{n_t}$ and m_t output variables $[y_{t1}, \dots, y_{tm}] = \mathbf{y}_t \in \mathbb{R}^{m_t}$. Two tasks $(\mathbf{x}_t, \mathbf{y}_t)$ and $(\mathbf{x}_{t'}, \mathbf{y}_{t'})$ are said to be *disjoint* if there is no overlap between their input and output variables: $(\{x_{ti}\}_{i=1}^{n_t} \cup \{y_{tj}\}_{j=1}^{m_t}) \cap (\{x_{t'i}\}_{i=1}^{n_{t'}} \cup \{y_{t'j}\}_{j=1}^{m_{t'}}) = \emptyset$.

The notion of word embeddings [4] can be extended to *variable embeddings* (VEs) [27] by treating the i -th variable as being associated with two elements:

- A specific *variable embedding* $\mathbf{z}_i \in \mathbb{R}^C$, which can be interpreted as the *name* or *key* of that variable. C is the dimensionality of the embedding.
- A specific scalar *value* $v_i \in \mathbb{R}$.

In particular, much like word embeddings, variable embeddings do not necessarily have to be specified in advance as they can be treated as parameters of a model and learned.

Let us describe a *prediction task* $(\mathbf{x}, \mathbf{y}) = ([x_1, \dots, x_n], [y_1, \dots, y_m])$. The goal is to predict the values of *target variables* $\{y_j\}_{j=1}^m$ (output) from the values of *observed variables* $\{x_i\}_{i=1}^n$ (input).

Notably, a *classification task* is a special case of a prediction task with target variables restricted to one-hot encodings.

A *predictor* Ω is a function which maps between observed and target variables. Let \mathbf{z}_i and \mathbf{z}_j be the variable embeddings of x_i and y_j . An MTL predictor can then be defined as:

$$\mathbb{E}[y_j|\mathbf{x}] = \Omega(\mathbf{x}, \{\mathbf{z}_i\}_{i=1}^n, \mathbf{z}_j) \quad (1)$$

Ω is shared across tasks to extract common knowledge and the tasks themselves are identified via their variable embeddings. A particular form of Ω is obtained by expressing the predictor via function composition:

$$\Omega(\mathbf{x}, \{\mathbf{z}_i\}_{i=1}^n, \mathbf{z}_j) = g\left(\sum_{i=1}^n f(x_i, \mathbf{z}_i), \mathbf{z}_j\right) \quad (2)$$

where f is an *encoder*, g is a *decoder*, and there is an implicit assumption that the ordering of observed variables does not matter. $f: \mathbb{R}^{C+1} \rightarrow \mathbb{R}^M$, $g: \mathbb{R}^{M+C} \rightarrow \mathbb{R}$, where M is the dimension of the latent space to which the encoder maps. f and g can be approximated with neural networks f_{θ_f} and g_{θ_g} where θ_f and θ_g are parameters learned by gradient descent.

The decoder can be further decomposed for computational efficiency:

$$\mathbb{E}[y_j|\mathbf{x}] = g_2\left(g_1\left(\sum_{i=1}^n f(x_i, \mathbf{z}_i)\right), \mathbf{z}_j\right) \quad (3)$$

where g_1 is the initial decoder which is independent of the target variable being predicted, while g_2 is the final decoder conditioned on the target variable's embedding. This allows g_1 to learn transformations of the observed variables not dependent on the specific output variable. Also, $g_1(\sum_{i=1}^n f(x_i, \mathbf{z}_i))$ can be pre-computed ahead of specific predictions for a given target variable.

As far as specific choices of architectures of the encoder and decoders are concerned, we follow the setup presented in [27] where the conditioning on variable embeddings is done via FiLM layers [31].

The described procedure shows specific advantages, e.g. the possibility to handle tasks with different dimensions of input and output spaces, the ability to recover structure on small-scale problems, and relatively good performance on a range of tasks. On the flip side, it does not reuse the obtained embeddings between variables and it does not lend itself readily to interpretation for real-world classification datasets. In principle, a variable embedding is obtained for each observed and target variable, so the embeddings can be compared in their common space or projected into a lower-dimension space for visualization using methods such as t-SNE [18] or UMAP [25]. In reality, however, this turns out to be problematic for more complex data. For instance, for the real world dataset of UCI-121 [12, 20], the vanilla variable embeddings approach produces embeddings which seem to differentiate between the observed variables, common target variables and uncommon target variables [27], but we do not have any more information on the relations between the variables themselves.

3 Method

In order to encourage the reuse of information between the variables and to increase the interpretability of the approach, we propose *shared variable embeddings*, selectively used for each observed variable. The outline of our method is shown in Figure 1.

3.1 Shared variable embeddings

Let us consider N observed variables and a set of D shared embeddings $\{\mathbf{s}_k\}_{k=1}^D$, with $\mathbf{s}_k \in \mathbb{R}^C$. The associated *shared embedding matrix* is $\mathbf{S}_{D \times C}$, where C is the dimension of both the embedding space of observed variables and the shared embedding space. In order to enforce the reuse of information between variable embeddings, we would like $D \ll N$. We relate the raw (initial) variable embeddings to the shared embeddings via attention.

For the *raw variable embedding matrix* $\mathbf{Z}_{N \times C}$, we follow the standard attention procedure [38]:

$$A(\mathbf{Q}, \mathbf{K}, \mathbf{V}) = \text{softmax}\left(\frac{\mathbf{Q}\mathbf{K}^T}{\sqrt{d_k}}\right) \mathbf{V} \quad (4)$$

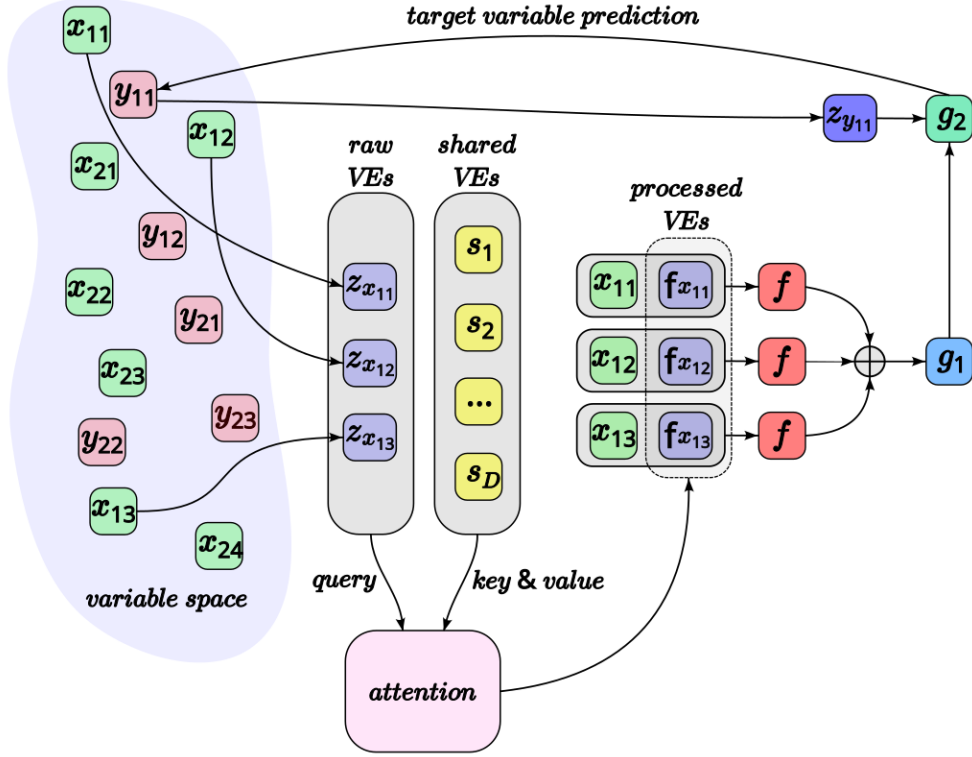


Figure 1: The overview of the *shared variable embeddings* method. The *variable space* contains both the *observed* and *target* variables which are associated with their learnable *variable embeddings* (VEs). The observable variables are first linked to *raw VEs* which are used as *queries* in the attention mechanism. A separate set of *shared VEs* plays the role of both *keys* and *values*. The *processed VEs* are the output of attention. Together with the corresponding variable values they are processed, each (value, VE) pair separately, by the *encoder*. The outputs of the encoder are summed and passed to the initial *decoder*. The target variable of interest is directly linked to its VE and this VE is passed with the output of the initial decoder to the final decoder to actually perform the prediction of the value of the target variable of interest. Additional details of the architecture are available in the Appendix in Figure 4.

where \mathbf{Q} , \mathbf{K} , \mathbf{V} can be interpreted as the matrices of *queries*, *keys* and *values*, respectively, and d is the dimensionality of both the queries and keys. In our specific case, we will apply cross-attention and the initial variable embeddings can be assigned the role of the queries, while the shared variable embeddings are assigned the roles of both the keys and the values:

$$A(\mathbf{Z}, \mathbf{S}, \mathbf{S}) = \text{softmax} \left(\frac{\mathbf{Z}\mathbf{S}^T}{\sqrt{C}} \right) \mathbf{S} \quad (5)$$

The output of this procedure is the *processed variable embedding matrix* $\mathbf{F}_{N \times C}$, where each *processed variable embedding* \mathbf{f}_i is a linear combination of all the shared embeddings, weighted by their similarity score to the *raw variable embedding* \mathbf{z}_i . Similarly to standard variable embeddings, shared variable embeddings can be either handcrafted or learned as model parameters.

Once the processed embedding has been obtained it can be substituted into Eq. 3 to get:

$$\mathbb{E}[y_j | \mathbf{x}] = g_2 \left(g_1 \left(\sum_{i=1}^n f(x_i, \mathbf{f}_i) \right), \mathbf{z}_j \right) \quad (6)$$

An important distinction between standard and shared variable embeddings is that the standard ones are inextricably tied to a specific variable from a specific dataset, while in our shared version each shared embedding is not directly linked to one specific variable from a given dataset and can be potentially reused between variables and datasets.

3.2 Training

The proposed model is trained end-to-end with stochastic gradient descent. For one training step, a two-fold procedure follows. First, a task is sampled from the distribution of overall tasks considered. Second, using the dataset associated with the sampled task, a sample of training examples is drawn. For each of these examples, standard variable embeddings are obtained for each of the observed and target variables. Those for the observed variables are passed through the attention mechanism to use the shared embeddings and obtain the processed variable embeddings. Such embeddings are then passed through the encoder/decoder architecture in order to obtain predictions for each target variable. These predictions are used to calculate the squared hinge loss:

$$L(\hat{\mathbf{y}}, \mathbf{t}) = \sum_{j=1}^m \max(0, 1 - t_j \cdot \hat{y}_j)^2 \quad (7)$$

where t_j is a $+1/-1$ encoding of the actual target and \hat{y}_j is the prediction of the value of the j -th target variable for the given task obtained from the encoder/decoder architecture with shared variable embeddings as in Eq. 6.

3.3 Imposing independence of shared variable embeddings through additional structure

One question that can be asked of the shared embedding matrix $\mathbf{S}_{D \times C}$ is that of structure. In particular, it could be argued that the learning process does not explicitly require the shared embeddings $\{\mathbf{s}_k\}_{k=1}^D$ to be *independent* from one another. We consider different notions of independence and several approaches to encourage it in the shared embeddings.

3.3.1 Orthogonalization

For a simple notion of independence, we consider an embedding independent from other embeddings when it is not a linear combination of them. With this, $r_{\mathbf{S}} = \text{rank}(\mathbf{S})$ is a measure of independence. In a realistic setting, we might still have $r_{\mathbf{S}} = C$ even if multiple embeddings are approximately linearly dependent. An operational measure of the rank of \mathbf{S} would require to address this drawback and we describe such a measure $q_{\mathbf{S}}$ in Section 3.3.2. The results from Section 4.2 show that the proposed training procedure results in $q_{\mathbf{S}} < C$. A straightforward way to build in more independence is to require \mathbf{S} to consist of *orthonormal* vectors. With an additional assumption of $D = C$, this would translate into an *orthogonality* requirement, which could be incorporated in the loss function:

$$L_{\text{orth}}(\hat{\mathbf{y}}, \mathbf{t}) = L(\hat{\mathbf{y}}, \mathbf{t}) + \alpha_{\text{orth}} \left(\sum_{i=j} (1 - \mathbf{D}_{i,j})^2 + \sum_{i \neq j} \mathbf{D}_{i,j}^2 \right) \quad (8)$$

where $\mathbf{D}_{C \times C} = \mathbf{S}^T \mathbf{S} = \mathbf{I}$. A subtle problem is that, for random initializations of \mathbf{S} , we might have $\det(\mathbf{S}^T \mathbf{S}) = -1$ and the optimization procedure may have trouble updating \mathbf{S} to obtain $\mathbf{S}^T \mathbf{S} \approx \mathbf{I}$. Because of that, the weight initialization procedure has to be adjusted so that $\det(\mathbf{S}^T \mathbf{S}) = 1$. This is done by only allowing random initializations which result in $\det(\mathbf{S}^T \mathbf{S}) = 1$.

3.3.2 Stable rank

Instead of focusing on restricting \mathbf{S} , it is possible to explicitly add $r_{\mathbf{S}}$ to the loss function. A significant drawback of this is the discontinuous characteristic of the rank measure, which makes it unsuitable for gradient descent. To address this, we rely on a continuous proxy. Let us consider a matrix $\mathbf{A}_{N \times M}$ with $\sigma_i(\mathbf{A})$ being its i -th *singular value*. The Frobenius norm of \mathbf{A} is defined as $\|\mathbf{A}\|_F^2 = \text{tr}(\mathbf{A} \mathbf{A}^T) = \sum_{i,j} \mathbf{A}_{i,j}^2 = \sum_i \sigma_i^2$. The *stable rank* [37] of \mathbf{A} is then defined as:

$$\text{sr}(\mathbf{A}) = \frac{\|\mathbf{A}\|_F^2}{\|\mathbf{A}\|^2} = \frac{\sum_i \sigma_i^2}{\max_i \sigma_i^2} \quad (9)$$

and $\text{sr}(\mathbf{A}) \leq \text{rank}(\mathbf{A})$.

For $q_{\mathbf{S}} = \text{sr}(\mathbf{S})$, the loss function can be extended:

$$L_{\text{sr}}(\hat{\mathbf{y}}, \mathbf{t}) = L(\hat{\mathbf{y}}, \mathbf{t}) + \alpha_{\text{sr}} (C - q_{\mathbf{S}}) \quad (10)$$

where C can be interpreted as the maximum possible rank of the shared embedding matrix.

3.3.3 Von Neumann entropy

It is possible to approach independence from the point of view of information theory. With this setup, *von Neumann entropy* could be used to nudge the shared embedding matrix to contain independent vector components. For a *density matrix* written in the basis of its eigenvectors, the von Neumann entropy is defined as:

$$V(\mathbf{A}) = - \sum_i \sigma_i^2 \ln \sigma_i^2 \quad (11)$$

Let $\mathbf{R}_{D \times C}$ be defined as \mathbf{S} normalized along the dimension of the shared embedding space, such that for the i -th row of \mathbf{R} we have $\sum_j \mathbf{R}_{i,j} = 1$. In other words, \mathbf{R} is the result of normalizing the rows of \mathbf{S} . Then, for $v_{\mathbf{R}} = V(\mathbf{R})$ we can modify the vanilla loss to make use of the von Neumann entropy:

$$L_{\text{vN}}(\hat{\mathbf{y}}, \mathbf{t}) = L(\hat{\mathbf{y}}, \mathbf{t}) - \alpha_{\text{vN}} v_{\mathbf{R}} \quad (12)$$

3.4 Sparse attention

In a procedure orthogonal to inducing structure in the shared embedding matrix, one can also restrict the way in which the actual shared embeddings are combined to form the processed embeddings. One drawback of the standard attention mechanism is that it assigns non-zero weights to all the value vectors. This means that even components with marginal similarity to the keys are present in the final linear combinations. A potential solution would be to make the output of the attention mechanism not rely on values with small similarity scores. In order to keep the whole mechanism differentiable, we adopt the α -entmax method [32]. Let us denote the d -probability simplex by $\triangle^d = \{\mathbf{p} \in \mathbb{R}^d : \mathbf{p} \geq 0, \|\mathbf{p}\|_1 = 1\}$. Sparsemax [23] is defined as:

$$\text{sparsemax}(\mathbf{z}) = \underset{\mathbf{p} \in \triangle^d}{\operatorname{argmin}} \|\mathbf{p} - \mathbf{z}\|^2 \quad (13)$$

A family of Tsallis α -entropies [36] can be defined for $\alpha \geq 1$ as:

$$H_{\alpha}^T(\mathbf{p}) = \begin{cases} \frac{1}{\alpha(1-\alpha)} \sum_j (p_j - p_j^{\alpha}), & \alpha \neq 1 \\ H^S(\mathbf{p}), & \alpha = 1 \end{cases} \quad (14)$$

where $H^S(\mathbf{p}) = - \sum_j p_j \ln p_j$.

Finally, the α -entmax, which can be understood as an interpolation between softmax and sparsemax, is defined as:

$$\alpha\text{-entmax}(\mathbf{z}) = \underset{\mathbf{p} \in \triangle^d}{\operatorname{argmax}} \mathbf{p}^T \mathbf{z} + H_{\alpha}^T(\mathbf{p}) \quad (15)$$

Given this definition, 1-entmax and 2-entmax are identical to softmax and sparsemax, respectively. α -entmax is differentiable, which also means that the value of the α parameter does not have to be supplied as a fixed hyperparameter as it can be learned together with other model parameters.

4 Experiments

We validate the ability of shared variable embeddings to solve real-life classification tasks and to help in interpretability on the UCI-121 [12, 20] dataset. In the experiments, we use the hyperparameter values and the learning setup from [27]. For the shared variable embeddings, we choose $D = C = 128$. We provide quantitative comparisons of the proposed method against a strong baseline: the variable embedding method without shared embeddings. We also consider the results with restrictions on the shared embedding matrix and on the attention mechanism, as proposed in Section 3. Additionally, we provide qualitative comparisons for the basic version of our method and for its configurations with constraints on the shared embedding matrix and with sparse attention.

4.1 Classification capability

Results in terms of best test set accuracy are presented in Table 1. We use the vanilla variable embedding method without shared embeddings [27] as a strong baseline. Quantitative assessment shows that the shared embedding approach is able to achieve a classification accuracy in the range of

Table 1: Best classification accuracy for variable embedding methods on the UCI-121 test set.

METHOD	ACCURACY	NO FINE-TUNING?
VANILLA	81.5	×
SHARED EMBEDDING	81.5	✓
1.05-ENTMAX	81.9	✓
STABLE RANK, $\alpha_{\text{sr}} = 0.05$	80.6	✓

the results from the baseline. At the same time, the 1.05-entmax sparse attention method is able to surpass the accuracy levels of both the baseline and the shared embedding method with full attention. Notably, the baseline requires additional fine-tuning on each of the 121 datasets while our approaches do not.

Details of the training process are displayed in Figure 2. Both the shared embedding method and the 1.05-entmax method show similar characteristics through the earlier part of the training process. A major difference, however, is that the entmax method hits the stop criterion significantly earlier and provides a higher final test set accuracy. The stable rank method with $\alpha_{\text{sr}} = 0.05$ hits visibly lower accuracy levels throughout training, while requiring more steps than the 1.05-entmax method. Figure 3a directly compares the number of steps before reaching the maximum test set accuracy. In particular, the 1.05-entmax model reaches its peak test set accuracy after 10,300 steps compared to 16,200 for the shared embedding method, which is a 36.4% decrease in training time measured in steps. The stable rank model with $\alpha_{\text{sr}} = 0.05$ requires 10,600 steps.

Ablation studies for methods involving orthogonalization, stable rank and von Neumann entropy as means to enforce independence in the shared embeddings are presented in Table 2. These results suggest that orthogonalization and, in particular, von Neumann entropy have an adverse effect on the final classification accuracy, while the stable rank restrictions do not seem to improve the results relative to straightforward shared embeddings but they do not decisively hurt them either.

An extensive ablation for the sparse attention methods is presented in Table 3. The α -entmax approaches are evaluated in two distinct settings. In the first one, α is picked as a hyperparameter, constant across the whole training procedure. In the second one, α is treated as a model parameter, with an initial value, and is optimized with gradient descent. In this case, the final optimized value of α is reported. The evaluations of the α -entmax methods show that it is important to adjust the weight initialization procedure of the model. For embeddings initialized as in the vanilla variable embedding approach, the final accuracy suffers. Increasing the standard deviation of the normal distribution from which the initial weights are sampled markedly improves the test accuracy. In particular, for the 1.05-entmax method with a standard normal distribution used for initialization, the accuracy reaches levels higher than for any other considered setup, with a significantly shortened training time. This suggests that for the particular tackled set of tasks, an attention mechanism with moderate induced sparsity provides slight advantages in terms of accuracy and significant advantages in terms of training time relative to the standard attention mechanism.

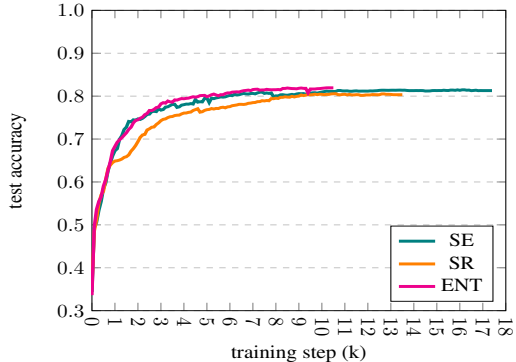


Figure 2: UCI-121 test set accuracy for a given train step (in thousands). SE - shared embedding method, ENT - 1.05-entmax with embeddings initialized from $\mathcal{N}(0, 1)$, SR - stable rank with $\alpha_{\text{sr}} = 0.05$.

4.2 Interpretability

To verify whether the introduction of shared embeddings $\{\mathbf{s}_k\}_{k=1}^D$ in fact generates reusable concepts and provides a degree of interpretability, we investigate their characteristics. The degree to which

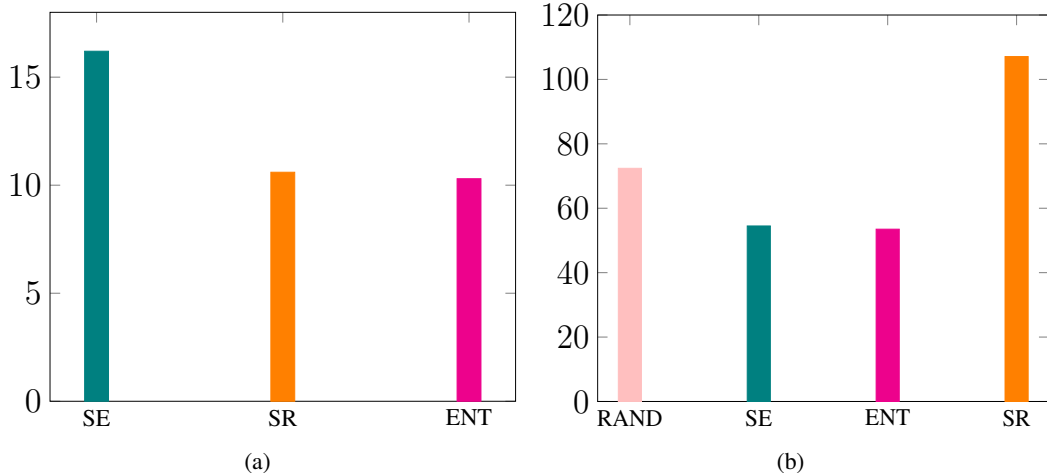


Figure 3: (a) Training steps needed to reach best test set accuracy. (b) Stable rank of the shared embedding matrix after training - best accuracy model. SE - shared embedding method, ENT - 1.05-entmax with embeddings initialized from $\mathcal{N}(0, 1)$, SR - stable rank with $\alpha_{sr} = 0.05$, RAND - random embedding matrix with entries from $\mathcal{N}(0, 1)$.

Table 2: Classification accuracy (ACC) for variable embedding methods with orthogonalization (left), stable rank (middle), von Neumann entropy (right) on the UCI-121 test set.

α_{ORTH}	ACC	α_{SR}	ACC	α_{VN}	ACC
0	75.5	0.01	79.9	0.001	68.6
0.1	74.5	0.04	80.3	0.01	67.8
1	74.3	0.05	80.3	0.05	71.9
10	72.4	0.06	80.7	0.5	69.6
100	74.3	0.1	79.0		
1000	71.4	0.5	79.7		
		1	76.2		

the shared embeddings are independent after training, as measured by stable rank, is presented in Figure 3b. The embeddings obtained from the straightforward shared embedding method and its version with sparse attention seem significantly less independent than random embeddings. On the flip side, the stable rank incarnation of our method is able to visibly increase the independence of the embeddings, as it directly optimizes for this goal.

We proceed to investigate whether this notion of independence correlates with the interpretability of specific shared embeddings. Towards this end, we propose an evaluation protocol for the ability of shared variable embeddings to differentiate between real-world concepts:

- Compute the attention scores for all raw variable embeddings.
- Sample s_p without repetition from the set of shared embeddings $\{s_k\}_{k=1}^D$.
- Select K variables from the given tasks whose raw variable embeddings are most similar to s_p .
- Verify whether the selected K variables map intuitively to one or more real-world concepts.

The variables most similar to a shared embedding representing a specific concept would be expected to share some intuitive notion, category or semantic meaning. In our evaluations, we choose $K = 5$. To aid in a quantitative as well as qualitative assessment of mapping to concepts, we introduce a measurable and less subjective assignment to real-world concepts in the form of the Subject Area ascribed to a given task/dataset in the UCI repository [20]. Each dataset has one Subject Area (SA) assigned to it from the following 11 possibilities: Biology (Bio), Business (Bus), Climate and Environment (C&E), Computer Science (CS), Engineering (E), Games (G), Health and Medicine

Table 3: Classification accuracy for variable embedding methods with α -entmax sparse attention on the UCI-121 test set. α represents the initial value used, while OPTIMIZED α is the final value of α for methods where α is treated as a model parameter.

α	CONTEXT STD	ACCURACY	OPTIMIZED α
0.5	1.0	79.7	0.91
0.9	1.0	81.1	0.83
1.05	0.01	80.9	1.74
1.05	0.05	78.8	1.58
1.05	0.1	80.9	1.62
1.05	0.5	81.1	1.36
1.05	1.0	81.9	1.00
1.05	2.0	76.0	0.88
1.5	0.1	78.9	1.76
1.5	0.5	80.8	×
1.5	1.0	77.0	×
1.5	1.0	78.6	1.36
1.5	1.0	80.8	1.38
2.0	1.0	75.2	×

Table 4: Most similar variables for a random choice of a shared embedding. Shared embedding method. Variables sorted in descending order of similarity. (-) denotes ambiguous data.

DATASET		VARIABLE MEANING	SA
MUSK (V2)		<i>A distance feature of a molecule along a ray.</i>	P&C
CONN. (S,MVR)	BENCH	<i>Energy within a particular frequency band, integrated over a certain period of time.</i>	P&C
WAVEFORM (V1)		<i>Waveform feature; contains noise but is not all noise.</i>	P&C
MINIBOONE		<i>A particle ID variable (real) for an event.</i>	P&C
ANNEALING		-	P&C

(H&M), Law (L), Physics and Chemistry (P&C), Social Sciences (SS) and Other (O). These categories afford us the option to measure the performance of a given model in terms of interpretability and compare it with other methods.

Table 4 and Table 5 show the results of running our evaluation procedure for one randomly chosen shared embedding. This consists of 5 variables most similar to the sampled shared embedding. We also present extended results where this procedure is repeated in Appendix A.

Table 4 suggests that the shared embedding method generates an embedding which is most similar to variables which have an intuitive interpretation of measuring physical quantities and phenomena. A quantitative analysis confirms this qualitative assessment. All identified variables belong to the Physics and Chemistry Subject Area. Also, all the variables come from distinct datasets. Qualitatively, these most similar variables represent quantities related to physical processes, e.g. energies, waveforms, as well as objects which such quantities describe: molecules, particles etc. They do seem to carry with them a distinct intuitive meaning. Both the quantitative and qualitative results indicate that the proposed method is able to identify concepts rather than tie the embeddings to specific datasets, contrary to what is the case for the standard variable embedding approach.

Table 5 shows a similar result for the 1.05-entmax sparse attention method. In this case, the majority of the selected variables seem to represent concepts related to health or biological systems. In quantitative terms, the majority belongs to one Subject Area - Health and Medicine, while there is also one variable identified as coming from the Biology Subject Area. The one variable which does not fit the health or biological interpretation is the least similar from the selected 5 and it belongs to the by-definition-broad Other category. Qualitatively, the most similar variables relate to living organisms. This is also the case for the fourth most similar variable from the Biology SA. We do, however, notice less internal consistency in this grouping, relative to the results from the base method.

Table 5: Most similar variables for a random choice of a shared embedding. 1.05-entmax sparse attention method with embeddings initialized from $\mathcal{N}(0, 1)$. Variables sorted in descending order of similarity. (-) denotes ambiguous data.

DATASET	VARIABLE MEANING	SA
BREAST CANCER WI (D.)	<i>Mean compactness of the cell nuclei in the image.</i>	H&M
THYROID DISEASE	-	H&M
ARRHYTHMIA	-	H&M
LEAVES (SHAPE)	<i>A specific feature relating to the shape of the leaf.</i>	BIO
SYNTH. CONTROL	<i>Point value on synthetically generated control chart.</i>	O

Table 6: Random choice of variables from the UCI-121 dataset. (-) denotes ambiguous data, (*) denotes inferred Subject Areas.

DATASET	VARIABLE MEANING	SA
AUDIOLOGY (S.)	-	H&M
-	-	BIO(*)
SYNTH. CONTROL	<i>Point value on synthetically generated control chart.</i>	O
TIC-TAC-TOE END.	<i>State of the bottom-left square at the end of a game.</i>	G
HEART DIS.	-	H&M

Both quantitative and qualitative results suggest that the base shared embedding method may actually produce more interpretable shared embeddings than the sparse attention approach. This is supported by repeat analysis presented in Appendix A where both methods seem to produce interpretable embeddings but the base method outperforms the sparse attention method in terms of the cohesion of the embeddings. The base method produces representations which are more easily linked to one broad intuitive concept while the inclusion of sparse attention prefers embeddings which are linked to more than one but still related concepts (e.g. biological and health-related ones).

While this investigation points to the relative performance of the methods, it is worth analyzing whether the results are not merely caused by the statistical characteristics of the dataset. To facilitate this, we replace the evaluation procedure with its random counterpart where we sample $K = 5$ variables from the UCI-121 dataset and perform the same qualitative and quantitative assessment as was the case for variables similar to the shared embedding from our models. The results for one such sample are presented in Table 6. There is one repeated category (H&M), however, it does not have a majority. Also, other than in some samples for the 1.05-entmax method, there is only one repeat category, not a contest between two categories. These indications also hold across additional samples presented in Appendix A. A further differentiating characteristic is that all the variables within each of the extended samples (in Appendix A) come from different datasets, whereas for our analyzed models datasets occasionally repeat. The only case when we observe a majority category for the random variables is one where these variables represent the Other SA, which is, by definition, a broad bracket in which we do not expect the variables to represent similar concepts. All this points to the fact that the most similar variables obtained from our models are significantly different from random choice.

4.3 Accuracy vs. interpretability trade-off

Drawing on the quantitative and qualitative results, we find that for our best performing methods none of them strictly dominates the other in terms of *both* accuracy and interpretability. The 1.05-entmax method achieves higher final accuracy than our base shared embedding method, 81.9% vs. 81.5%. On the flip side, the base shared embedding method does seem to more successfully separate real-world concepts into specific shared embeddings. Specifically, in our extended results (Appendix A), we see

that the base shared embedding method achieves more consistent concept assignment to the shared embeddings. For 5 trials, we obtain 3 where there is a majority SA. In one trial, there was no majority but there was a dominant SA without draws. One trial resulted in a draw between SAs. It is also worth noting that for one trial, all the similar variables come from the same SA (P&C) and from different datasets. Conversely, for the 1.05-entmax method, the assignment of shared embeddings to concepts is still present, only weaker. One trial results in a majority SA assignment (H&M). 3 trials end in draws between dominant categories. Importantly, one trial has all the similar variables represent different SAs from distinct datasets. With these results, there seems to be a trade-off between prediction accuracy and interpretability.

5 Conclusion

We have proposed a new variable embedding architecture for general prediction problems. This architecture is based on shared embeddings with attention, which is a lightweight addition to the variable embedding architecture. We have considered several potential versions of this approach, introducing restrictions on the shared embeddings and adding sparsity to the attention mechanism. Other than in the standard variable embedding method, our approach does not require one variable embedding to represent one specific variable from a concrete dataset, but rather encourages the reuse of shared embeddings among variables across distinct datasets.

In empirical experiments, we have shown that our base method performs as well as the standard variable embedding method on the UCI-121 dataset, while not requiring any fine-tuning, which the standard method does. Additionally, we have performed a series of ablations to identify which versions of our architecture perform favorably in terms of classification accuracy and the potential interpretability of the shared embeddings. The results have demonstrated that the sparse attention mechanism helps in: (1) achieving superior classification performance and (2) requiring significantly less training steps than our base method. However, the gain comes at a cost of decreased interpretability relative to our base shared embedding method. This suggests a potential trade-off between performance and interpretability.

As far as interpretability itself is concerned, both our base method and its extension with sparse attention are able to use the shared embeddings to identify abstract concepts instead of making hard links to concrete variables from specific datasets, which is the case for the standard variable embedding approach. The base shared embedding method generates embeddings which are more interpretable and internally consistent than the sparse attention modification.

Given the results we have obtained, several lines of enquiry emerge: (1) investigation of other methods to restrict the shared embedding space, e.g. based on quantization, (2) adaptation of the variable embedding method and the shared embedding approach to vision, (3) use of *self-supervised learning* for the shared embeddings approach.

References

- [1] M. Assran, Q. Duval, I. Misra, P. Bojanowski, P. Vincent, M. Rabbat, Y. LeCun, and N. Ballas. Self-supervised learning from images with a joint-embedding predictive architecture. In *Proceedings of the IEEE/CVF Conference on Computer Vision and Pattern Recognition (CVPR)*, pages 15619–15629, June 2023.
- [2] D. Bahdanau, K. Cho, and Y. Bengio. Neural machine translation by jointly learning to align and translate. In Y. Bengio and Y. LeCun, editors, *3rd International Conference on Learning Representations, ICLR 2015, San Diego, CA, USA, May 7-9, 2015, Conference Track Proceedings*, 2015.
- [3] A. Bardes, J. Ponce, and Y. LeCun. VICReg: Variance-invariance-covariance regularization for self-supervised learning. In *International Conference on Learning Representations*, 2022.
- [4] Y. Bengio, R. Ducharme, and P. Vincent. A neural probabilistic language model. In T. K. Leen, T. G. Dietterich, and V. Tresp, editors, *NIPS*, pages 932–938. MIT Press, 2000.
- [5] D. Brügemann, M. Kanakis, A. Obukhov, S. Georgoulis, and L. Van Gool. Exploring relational context for multi-task dense prediction. In *Proceedings of the IEEE/CVF International Conference on Computer Vision (ICCV)*, pages 15869–15878, October 2021.

- [6] R. Caruana. Multitask learning: A knowledge-based source of inductive bias. In *Proceedings of the Tenth International Conference on Machine Learning*, ICML'93, page 41–48, San Francisco, CA, USA, 1993. Morgan Kaufmann Publishers Inc.
- [7] R. Caruana. Learning many related tasks at the same time with backpropagation. In G. Tesauro, D. Touretzky, and T. Leen, editors, *Advances in Neural Information Processing Systems*, volume 7. MIT Press, 1994.
- [8] R. Caruana. Algorithms and applications for multitask learning. In *International Conference on Machine Learning*, 1996.
- [9] R. Caruana. Multitask learning. *Machine Learning*, 28:41–75, 1997.
- [10] T. Chen, S. Kornblith, M. Norouzi, and G. Hinton. A simple framework for contrastive learning of visual representations. In H. D. III and A. Singh, editors, *Proceedings of the 37th International Conference on Machine Learning*, volume 119 of *Proceedings of Machine Learning Research*, pages 1597–1607. PMLR, 13-18 Jul 2020.
- [11] Z. Cui, G.-J. Qi, L. Gu, S. You, Z. Zhang, and T. Harada. Multitask act with orthogonal tangent regularity for dark object detection. In *Proceedings of the IEEE/CVF International Conference on Computer Vision (ICCV)*, pages 2553–2562, October 2021.
- [12] M. Fernández-Delgado, E. Cernadas, S. Barro, and D. Amorim. Do we need hundreds of classifiers to solve real world classification problems? *Journal of Machine Learning Research*, 15(90):3133–3181, 2014.
- [13] K. Fukushima. Neocognitron: A self-organizing neural network model for a mechanism of pattern recognition unaffected by shift in position. *Biological Cybernetics*, 36:193–202, 1980.
- [14] Y. Gao, J. Ma, M. Zhao, W. Liu, and A. L. Yuille. Nddr-cnn: Layerwise feature fusing in multitask cnns by neural discriminative dimensionality reduction. In *Proceedings of the IEEE/CVF Conference on Computer Vision and Pattern Recognition (CVPR)*, June 2019.
- [15] A. Goyal, A. Lamb, J. Hoffmann, S. Sodhani, S. Levine, Y. Bengio, and B. Schölkopf. Recurrent independent mechanisms. In *International Conference on Learning Representations*, 2021.
- [16] A. Graves, G. Wayne, and I. Danihelka. Neural turing machines. *arXiv:1410.5401*, 2014.
- [17] A. Graves, G. Wayne, M. Reynolds, T. Harley, I. Danihelka, A. Grabska-Barwińska, S. G. Colmenarejo, E. Grefenstette, T. Ramalho, J. Agapiou, A. P. Badia, K. M. Hermann, Y. Zwols, G. Ostrovski, A. Cain, H. King, C. Summerfield, P. Blunsom, K. Kavukcuoglu, and D. Hassabis. Hybrid computing using a neural network with dynamic external memory. *Nature*, 538(7626):471–476, Oct. 2016.
- [18] G. E. Hinton and S. Roweis. Stochastic neighbor embedding. In S. Becker, S. Thrun, and K. Obermayer, editors, *Advances in Neural Information Processing Systems*, volume 15. MIT Press, 2002.
- [19] R. Hu and A. Singh. Unit: Multimodal multitask learning with a unified transformer. In *Proceedings of the IEEE/CVF International Conference on Computer Vision (ICCV)*, pages 1439–1449, October 2021.
- [20] M. Kelly, R. Longjohn, and K. Nottingham. The uci machine learning repository, 2023.
- [21] Y. LeCun, B. Boser, J. S. Denker, D. Henderson, R. E. Howard, W. Hubbard, and L. D. Jackel. Backpropagation applied to handwritten zip code recognition. *Neural Computation*, 1:541–551, 1989.
- [22] M. Mahmud and S. Ray. Transfer learning using kolmogorov complexity: Basic theory and empirical evaluations. In J. Platt, D. Koller, Y. Singer, and S. Roweis, editors, *Advances in Neural Information Processing Systems*, volume 20. Curran Associates, Inc., 2007.
- [23] A. F. T. Martins and R. F. Astudillo. From softmax to sparsemax: A sparse model of attention and multi-label classification. In *Proceedings of the 33rd International Conference on Machine Learning - Volume 48*, ICML'16, page 1614–1623. JMLR.org, 2016.

- [24] W. McCulloch and W. Pitts. A logical calculus of ideas immanent in nervous activity. *Bulletin of Mathematical Biophysics*, 5:127–147, 1943.
- [25] L. McInnes, J. Healy, and J. Melville. Umap: Uniform manifold approximation and projection for dimension reduction. *arXiv:1802.03426*, Feb. 2018.
- [26] E. Meyerson and R. Miikkulainen. Modular universal reparameterization: Deep multi-task learning across diverse domains. In H. Wallach, H. Larochelle, A. Beygelzimer, F. d'Alché-Buc, E. Fox, and R. Garnett, editors, *Advances in Neural Information Processing Systems*, volume 32. Curran Associates, Inc., 2019.
- [27] E. Meyerson and R. Miikkulainen. The traveling observer model: Multi-task learning through spatial variable embeddings. In *International Conference on Learning Representations*, 2021.
- [28] T. Mikolov, K. Chen, G. Corrado, and J. Dean. Efficient estimation of word representations in vector space. In Y. Bengio and Y. LeCun, editors, *1st International Conference on Learning Representations, ICLR 2013, Scottsdale, Arizona, USA, May 2-4, 2013, Workshop Track Proceedings*, 2013.
- [29] I. Misra, A. Shrivastava, A. Gupta, and M. Hebert. Cross-stitch networks for multi-task learning. In *Proceedings of the IEEE Conference on Computer Vision and Pattern Recognition (CVPR)*, June 2016.
- [30] V. Mnih, K. Kavukcuoglu, D. Silver, A. A. Rusu, J. Veness, M. G. Bellemare, A. Graves, M. Riedmiller, A. K. Fidjeland, G. Ostrovski, S. Petersen, C. Beattie, A. Sadik, I. Antonoglou, H. King, D. Kumaran, D. Wierstra, S. Legg, and D. Hassabis. Human-level control through deep reinforcement learning. *Nature*, 518(7540):529–533, 2015.
- [31] E. Perez, F. Strub, H. de Vries, V. Dumoulin, and A. C. Courville. Film: Visual reasoning with a general conditioning layer. In *AAAI*, 2018.
- [32] B. Peters, V. Niculae, and A. F. T. Martins. Sparse sequence-to-sequence models. In A. Korhonen, D. Traum, and L. Màrquez, editors, *Proceedings of the 57th Annual Meeting of the Association for Computational Linguistics*, pages 1504–1519, Florence, Italy, July 2019. Association for Computational Linguistics.
- [33] R. Rombach, A. Blattmann, D. Lorenz, P. Esser, and B. Ommer. High-resolution image synthesis with latent diffusion models. In *Proceedings of the IEEE/CVF Conference on Computer Vision and Pattern Recognition (CVPR)*, pages 10684–10695, June 2022.
- [34] F. Rosenblatt. The perceptron: A probabilistic model for information storage and organization in the brain. *Psychological Review*, 65(6):386–408, 1958.
- [35] S. Thrun and J. O’Sullivan. Discovering structure in multiple learning tasks: The TC algorithm. In L. Saitta, editor, *Proceedings of the 13th International Conference on Machine Learning ICML-96*, San Mateo, CA, 1996. Morgan Kaufmann.
- [36] C. Tsallis. Possible generalization of boltzmann-gibbs statistics. *Journal of Statistical Physics*, 52:479–487, 1988.
- [37] L. Vasershtein. Stable rank of rings and dimensionality of topological spaces. *Functional Analysis and Its Applications*, 5:102–110, 1971.
- [38] A. Vaswani, N. Shazeer, N. Parmar, J. Uszkoreit, L. Jones, A. N. Gomez, L. u. Kaiser, and I. Polosukhin. Attention is all you need. In I. Guyon, U. V. Luxburg, S. Bengio, H. Wallach, R. Fergus, S. Vishwanathan, and R. Garnett, editors, *Advances in Neural Information Processing Systems*, volume 30. Curran Associates, Inc., 2017.
- [39] H. Ye and D. Xu. Taskprompter: Spatial-channel multi-task prompting for dense scene understanding. In *The Eleventh International Conference on Learning Representations*, 2023.
- [40] J. Zbontar, L. Jing, I. Misra, Y. LeCun, and S. Deny. Barlow twins: Self-supervised learning via redundancy reduction. In M. Meila and T. Zhang, editors, *Proceedings of the 38th International Conference on Machine Learning*, volume 139 of *Proceedings of Machine Learning Research*, pages 12310–12320. PMLR, 18–24 Jul 2021.

A Extended interpretability results.

While the samples presented in the main paper are instructive of the ability of our models to produce interpretable shared embeddings and of the difference between them and a random assignment, it is important to present and analyze a larger number of samples. Additional samples for (a) the base shared embedding method, (b) the 1.05-entmax sparse attention method and (c) random choice are presented below in Tables 7, 8, 9. For each method, the analysis encompasses 5 trials. In each trial, a shared embedding is chosen at random without replacement. For the base shared embedding method and the 1.05-entmax method, 5 variables most similar to the chosen random shared embedding are presented. The similarity between the sampled shared embedding \mathbf{s}_p and the i -th variable is measured as the cosine similarity S_C between the shared embedding and the processed variable embedding \mathbf{f}_i associated with this specific variable:

$$S_C(\mathbf{s}_p, \mathbf{f}_i) = \frac{\mathbf{s}_p \cdot \mathbf{f}_i}{\|\mathbf{s}_p\| \|\mathbf{f}_i\|} \quad (16)$$

For the random choice setup, a random choice without replacement of 5 variables is shown.

A.1 Shared embedding method

Trials (Table 7):

1. All the selected variables come from the same Subject Area (SA), Physics and Chemistry. Also, all the variables come from distinct datasets. This supports the view that the shared embedding method is able to identify the underlying abstract concepts behind the variables and does not necessarily form a very strong link between the shared embeddings and specific datasets. Qualitatively, the identified variables show a relatively consistent intuitive concept related to the measurement of physical phenomena or objects.
2. 3 variables come from the Biology SA, which forms the dominant category. The remaining 2 variables come from the Physics and Chemistry SA. There are 4 datasets represented, which shows that the shared embeddings are not strongly linked to specific datasets. Qualitatively, the chosen variables do represent an intuitive abstract concept related to biological phenomena. It can also be argued that the physical variables present in the choice describe natural phenomena, which, together with the biological variables, would form a relatively consistent grouping.
3. There is a dominant category with 4 variables in the form of Health and Medicine. All the selected variables come from different datasets. There is significant coherence to the grouping, which can also be seen in qualitative terms as the only physical variable in the selection can still be understood as describing elements of a real-world structure, similar to most of the biological variables. All in all, an intuitive biological concept can be identified.
4. There is a dominant category, Health and Medicine, albeit not a majority category. There are 4 distinct SA represented and 4 datasets. The majority of the selected variables can still intuitively be interpreted as ones related to health or the biological functioning of organisms, but outliers such as values from synthetically generated charts are also present. Overall, the interpretation is made significantly harder by ambiguous data.
5. The dominant SA, Physics and Chemistry, is represented by 2 variables, so there is no majority SA, and also it is tied with Health and Medicine for the number of variables. All variables come from distinct datasets. Other than in other trials, there is a more clear split of meaning between two concepts: physical and health-related ones. There is still some intuitive overlap but the internal consistency of the variables is weaker than for the other trials.

Overall, the shared embedding method results in similar variables which have a majority SA in 3/5 trials, a dominant category without ties in 4/5 trials and a dominant category with possible draws in all 5/5 trials. Also, there is at most one repeated dataset in any of the trials. If we were to adopt a view that different versions of the same dataset effectively count as one dataset, then we would only have one trial (2) with two repeated datasets. Qualitatively, all the the selected trials display the potential of the method to identify abstract concepts from varied areas.

Table 7: Most similar variables from the UCI-121 dataset for a random choice of a shared embedding. Shared embedding method. Variables sorted in descending order of similarity. Missing values (-) denote ambiguous data. (*) denotes inferred Subject Areas. The *Remarks* column lists the most dominant Subject Area (SA), the number of SAs present and the number of distinct datasets represented.

NO.	DATASET	VARIABLE MEANING	SUBJECT AREA	REMARKS
(1)	MUSK (V2)	<i>A distance feature of a molecule along a ray.</i>	PHYSICS AND CHEMISTRY	DOM.: 5/5 SAS: 1 D-SETS: 5
	C. BENCH (S,MVSR)	<i>Energy within a frequency band, integrated over time.</i>	PHYSICS AND CHEMISTRY	
	WAVEFORM (V1)	<i>Waveform feature; contains noise but is not all noise.</i>	PHYSICS AND CHEMISTRY	
	MINIBOONE	<i>A particle ID variable (real) for an event.</i>	PHYSICS AND CHEMISTRY	
	ANNEALING	-	PHYSICS AND CHEMISTRY	
(2)	-	-	BIOLOGY(*)	DOM.: 3/5 SAS: 2 D-SETS: 4
	MUSK (V2)	<i>A distance feature of a molecule along a ray.</i>	PHYSICS AND CHEMISTRY	
	LEAVES (SHAPE)	<i>A specific feature relating to the shape of the leaf.</i>	BIOLOGY	
	MUSK (V1)	<i>A distance feature of a molecule along a ray.</i>	PHYSICS AND CHEMISTRY	
	LEAVES (SHAPE)	<i>A specific feature relating to the shape of the leaf.</i>	BIOLOGY	
(3)	DERMATOLOGY	<i>Thinning of the suprapapillary epidermis.</i>	HEALTH AND MEDICINE	DOM.: 4/5 SAS: 2 D-SETS: 5
	SPECT HEART	<i>Binary feature of cardiac CT images.</i>	HEALTH AND MEDICINE	
	MINIBOONE	<i>A particle ID variable (real) for an event</i>	PHYSICS AND CHEMISTRY	
	HABERMAN	<i>Number of positive axillary nodes detected.</i>	HEALTH AND MEDICINE	
	HEART DIS. (CH)	-	HEALTH AND MEDICINE	
(4)	ARRHYTHMIA	-	HEALTH AND MEDICINE	DOM.: 2/5 SAS: 4 D-SETS: 4
	-	-	BIOLOGY(*)	
	ARRHYTHMIA	-	HEALTH AND MEDICINE	
	SYNTH. CONTROL	<i>Point value on synthetically generated control chart.</i>	OTHER	
	MINIBOONE	<i>A particle ID variable (real) for an event</i>	PHYSICS AND CHEMISTRY	
(5)	ANNEALING	-	PHYSICS AND CHEMISTRY	DOM.: 2/5 SAS: 3 D-SETS: 5
	BREAST CANCER	<i>Whether irradiation was used.</i>	HEALTH AND MEDICINE	
	OR OF H. DIGITS	<i>Preprocessed feature of a digit image.</i>	COMPUTER SCIENCE	
	MUSK (V2)	<i>A distance feature of a molecule along a ray.</i>	PHYSICS AND CHEMISTRY	
	PRIMARY TUMOR	<i>Whether sample is related to supraclavicular LNs.</i>	HEALTH AND MEDICINE	

A.2 1.05-entmax method

Trials (Table 8):

1. 3 variables come from the Health and Medicine SA and form a dominant category. All the variables are from distinct datasets. Quantitatively, the method shows potential to identify notions related to health. The qualitative analysis is hindered by the ambiguity of the data, however, one might still identify an intuitive concept relating to diseases or a broader one relating to living organisms.
2. A failure case: all the variables are from different SA and so, there is no reliable dominant category. All the variables come from distinct datasets. For this specific trial, no underlying concept can be easily identified.
3. There is a dominant category, Physics and Chemistry, with 2 variables, but it is tied for the lead with another SA, Health and Medicine, in terms of the number of identified variables. All the selected variables come from distinct datasets. There are two underlying intuitive concepts: a physical one and one related to health.
4. We do have a dominant SA, Biology, with 2 variables, but again, there is another category with the same number of identified variables - Health and Medicine. Also, we see that for this trial, there are 2 repeated datasets. The intuitive meaning behind the variables from this trial can be interpreted as describing living things but more details are occluded by the fact that all the variables for the Health and Medicine SA are ambiguous.
5. Biology is the dominant category with 2 representatives, but the Health and Medicine SA has the same number of identified variables. All the variables come from distinct datasets. Qualitatively, the underlying concept can be identified as a description of a real-world structure or a point on a larger representation of a phenomenon. With this interpretation, even the variable coming from the Other SA fits the concept.

The 1.05-entmax sparse attention method identifies variables in a distinctly different way than the base shared embedding method. Namely, there are far less cases with majority SAs and far more outcomes where the dominant category is tied for the lead with another SA as far as the number of identified variables is concerned. The sparse attention method still prefers variables from distinct datasets and does not seem to very strongly link a particular shared embedding to a concrete dataset. At the same time, both the quantitative metrics and the qualitative assessment suggest that it is the base shared embedding method that more successfully delineates between abstract concepts.

Table 8: Most similar variables from the UCI-121 dataset for a random choice of a shared embedding. 1.05-entmax sparse attention method with embeddings initialized from $\mathcal{N}(0, 1)$. Variables sorted in descending order of similarity. Missing values (-) denote ambiguous data. (*) denotes inferred Subject Areas. The *Remarks* column lists the most dominant Subject Area (SA), the number of SAs present and the number of distinct datasets represented.

NO.	DATASET	VARIABLE MEANING	SUBJECT AREA	REMARKS
(1)	BR. CANCER WI (D.)	<i>Mean compactness of the cell nuclei in the image.</i>	HEALTH AND MEDICINE	DOM.: 3/5 SAS: 3 D-SETS: 5
	THYROID DISEASE	-	HEALTH AND MEDICINE	
	ARRHYTHMIA	-	HEALTH AND MEDICINE	
	LEAVES (SHAPE)	<i>A specific feature relating to the shape of the leaf.</i>	BIOLOGY	
	SYNTH. CONTROL	<i>Point value on synthetically generated control chart.</i>	OTHER	
(2)	-	-	BIOLOGY(*)	DOM.: 1/5 SAS: 5 D-SETS: 5
	CONNECT-4	<i>Which of the players has taken position d5.</i>	GAMES	
	SYNTH. CONTROL	<i>Point value on synthetically generated control chart.</i>	OTHER	
	ARRHYTHMIA	-	HEALTH AND MEDICINE	
	MUSK (V2)	<i>A distance feature of a molecule along a ray.</i>	PHYSICS AND CHEMISTRY	
(3)	MUSK (V1)	<i>A distance feature of a molecule along a ray.</i>	PHYSICS AND CHEMISTRY	DOM.: 2/5 SAS: 3 D-SETS: 5
	WINE	<i>Flavanoids.</i>	PHYSICS AND CHEMISTRY	
	STATLOG (V. SILH.)	<i>Elongatedness of a silhouette of a vehicle.</i>	OTHER	
	BR. CANCER WI (P.)	<i>Mean texture of the cell nuclei in the image.</i>	HEALTH AND MEDICINE	
	ARRHYTHMIA	-	HEALTH AND MEDICINE	
(4)	LEAVES (SHAPE)	<i>A specific feature relating to the shape of the leaf.</i>	BIOLOGY	DOM.: 2/5 SAS: 3 D-SETS: 3
	ARRHYTHMIA	-	HEALTH AND MEDICINE	
	ARRHYTHMIA	-	HEALTH AND MEDICINE	
	LEAVES (SHAPE)	<i>A specific feature relating to the shape of the leaf.</i>	BIOLOGY	
	C. BENCH (S,MvsR)	<i>Energy within a frequency band, integrated over time.</i>	PHYSICS AND CHEMISTRY	
(5)	HORSE COLIC	<i>Temperature of extremities.</i>	BIOLOGY	DOM.: 2/5 SAS: 3 D-SETS: 5
	MOL. BIOL. (PGS)	<i>Position -50 in the DNA sequence.</i>	BIOLOGY	
	LUNG CANCER	-	HEALTH AND MEDICINE	
	SYNTH. CONTROL	<i>Point value on synthetically generated control chart.</i>	OTHER	
	HEART DIS. (VALB)	<i>Maximum heart rate achieved.</i>	HEALTH AND MEDICINE	

A.3 Random choice

In order to account for the statistical properties of the UCI-121 dataset, we perform an analysis where the selected variables are actually randomly sampled without repetition from the dataset. If the dataset is not heavily skewed toward the concepts identified by either of our methods, it is natural to assume that we will see a lot more variability in the selection. For a random choice of variables, one could expect not to see majority SAs, or at least see them infrequently. Similarly, the expectation would be to see more SAs within each trial than is the case for our methods. Also, a random assignment would result in very frequent situations where all the variables come from distinct datasets. Conversely, for the base shared embedding method and the 1.05-entmax method the expectation would be that the variables most similar to a given shared embedding would be more likely to come from the same dataset. Table 9 summarizes the results for the random choice of variables. Indeed, there is only one trial with a majority category, but on inspection the identified SA is Other, which is a blanket category for a range of datasets representing different concepts. Apart from this special case, there are no other majority categories in trials. This suggests significantly weaker interpretability than for the base shared embedding method. The sparse attention method does show similar levels of dominant categories, however, with a crucial distinction. In the sparse attention approach, all the non-majority cases bar one had a tie for the dominant category, suggesting that the method was able to identify concepts better than random choice, with the assignment to two competing concepts. For random choice, such a competing assignment does not occur. Also, there are visibly more SAs represented than for the shared embedding method. Qualitatively, random choice does result in an assortment of

Table 9: Random choice of variables from the UCI-121 dataset. Missing values (-) denote ambiguous data. (*) denotes inferred Subject Areas. The *Remarks* column lists the most dominant Subject Area (SA), the number of SAs present and the number of distinct datasets represented.

NO.	DATASET	VARIABLE MEANING	SUBJECT AREA	REMARKS
(1)	AUDIOLOGY (S.)	-	HEALTH AND MEDICINE	DOM.: 2/5 SAS: 4 D-SETS: 5
	-	-	BIOLOGY(*)	
	SYNTH. CONTROL	Point value on synthetically generated control chart.	OTHER	
	TIC-TAC-TOE END.	State of the bottom-left square at the end of a game.	GAMES	
	HEART DIS. (CH)	-	HEALTH AND MEDICINE	
(2)	C. BENCH (S,MvsR)	Energy within a frequency band, integrated over time.	PHYSICS AND CHEMISTRY	DOM.: 2/5 SAS: 4 D-SETS: 5
	MUSK (V2)	A distance feature of a molecule along a ray.	PHYSICS AND CHEMISTRY	
	STATLOG (IMAGE S.)	-	OTHER	
	YEAST	Score of discriminant analysis of proteins.	BIOLOGY	
	ARRHYTHMIA	-	HEALTH AND MEDICINE	
(3)	MOL. BIOL. (SGS)	Position +23 in the DNA sequence.	BIOLOGY	DOM.: 2/5 SAS: 3 D-SETS: 5
	MUSK (V2)	A distance feature of a molecule along a ray.	PHYSICS AND CHEMISTRY	
	OZONE LEVEL	Precipitation.	CLIMATE AND ENV.	
	SOYBEAN (LARGE)	Type of seed treatment (e.g. fungicide).	BIOLOGY	
	LR SPECTROMETER	Specific flux measurement for the red band.	PHYSICS AND CHEMISTRY	
(4)	LIBRAS MOVEMENT	Coordinate abscissa of the 19th point.	OTHER	DOM.: 3/5 SAS: 2 D-SETS: 5
	ARRHYTHMIA	-	HEALTH AND MEDICINE	
	PITTSBURGH BRIDGES	Purpose of the bridge.	OTHER	
	TRAINS	-	OTHER	
	DERMATOLOGY	Clinical attributes: definite borders.	HEALTH AND MEDICINE	
(5)	MUSK (V1)	A distance feature of a molecule along a ray.	PHYSICS AND CHEMISTRY	DOM.: 2/5 SAS: 3 D-SETS: 5
	-	-	BIOLOGY(*)	
	HABERMAN	Number of positive axillary nodes detected.	HEALTH AND MEDICINE	
	MUSK (V2)	A distance feature of a molecule along a ray.	PHYSICS AND CHEMISTRY	
	MOL. BIOL. (PGS)	Position -22 in the DNA sequence.	BIOLOGY	

more than two distinct concepts for a given trail rather than in the identification of an abstract notion or two such notions, which is a frequent situation for the shared embedding method and 1.05-entmax methods.

B Architecture of the proposed method.

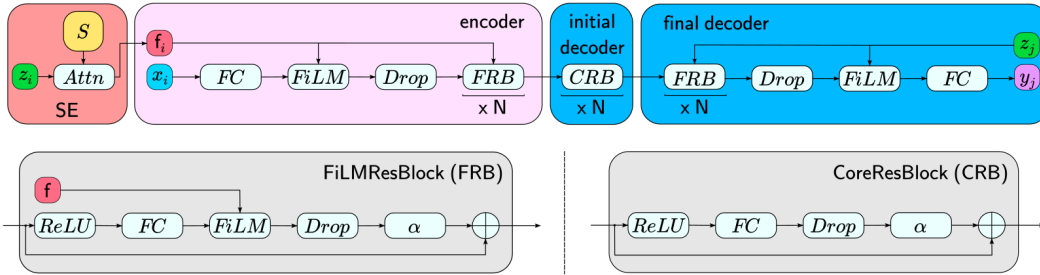


Figure 4: Architecture of the *shared variable embeddings* method. SE - shared embeddings, Attn - attention, S - shared embedding matrix, FC - fully connected layers, FiLM - layers proposed by [31], Drop - dropout, ReLU - rectified linear units.